Seismic behavior comparison of RC shear walls strengthened using FRP composites and steel elements

Omid Habibi [a], Alireza Khaloo [a,*], Hatef Abdoos [a]

[a] *Department of Civil Engineering, Sharif University of Technology, Tehran, Iran.*

Abstract

This paper aims at investigating the seismic behavior of strengthened reinforced concrete (RC) shear walls using a 3D finite element analysis. A series of four different configurations of carbon fiber reinforced polymer (CFRP) composites and four different schemes of steel elements are utilized to compare the two methods of retrofitting RC shear walls with similar dimensions and reinforcement ratios. Nonlinear simulations of the RC shear walls are conducted under the action of lateral cyclic loading in ABAQUS Explicit software. In addition, the numerical modeling for RC walls strengthened by CFRP composites as well as steel elements are validated according to the previous experimental studies. The numerical results reveal that both types of strengthening methods have desirable performance in terms of the ultimate load capacity, failure displacement, energy absorption, and ductility in comparison with the control shear wall (CSW). Furthermore, evaluation of the response parameters including secant stiffness and dissipated energy demonstrate that utilizing steel elements is more advantageous compared to CFRP composites.

Keywords: RC shear wall, Finite element, CFRP, Steel elements, Strengthening, Dissipated energy, Ductility, Secant stiffness.

[*]. Corresponding author. Tel: +98 21 66164211

E-mail address: khaloo@sharif.edu (A. R. Khaloo); omidhabi@gmail.com (O. Habibi); abdoos_hatef@yahoo.com (H. Abdoos)

Nomenclature

d_c	Softening coefficients in compression
d_t	Softening coefficients in tension
Δ_y	Yield displacement
Δ_u	Ultimate displacement
k	Ratio of second stress invariant on the tensile meridian to that on the compressive meridian
K_i	Secant stiffness corresponding to the loading cycle *i*
σ_{True}	True stress
σ_{Eng}	Engineering stress
ε_{Eng}	Engineering strain
ε_{True}	True strain
σ_c	Compressive stress
σ_t	Tensile stress
σ_{cu}	Maximum compressive stress
σ_{tu}	Maximum tensile stress
F_i	Maximum load corresponding to the loading cycle *i*
E	Young' modulus
$\varepsilon_c^{in,h}$	Inelastic strain
$\varepsilon_c^{pl,h}$	Plastic strain
$\varepsilon_t^{ck,h}$	Crack strain
$\varepsilon_t^{pl,h}$	Plastic strain
μ	Ductility
X_i	Maximum displacement corresponding to the loading cycle *i*

1. Introduction

Reinforced concrete (RC) shear walls are conventional structural elements incorporated in seismic regions to improve the strength and rigidity of structures against lateral loading (earthquake and wind forces). Limitation of lateral deformations along with minimizing damage to structural/non-structural components are the main advantages of RC shear walls owing to the significant in-plane stiffness.

A number of designed shear walls suffer from deficiencies including inadequate stiffness, insufficient reinforcements, and undesirable wall dimensions, which affects the performance of RC walls under the lateral loading. Additionally, avoid brittle shear failure of RC walls, not only sufficient stiffness but also adequate ductility needs to be provided. Therefore, investigating the strengthening methods considering various parameters for retrofitting of existing RC shear walls is of fundamental importance. The examination of strengthening methods can be categorized into the experimental observations and numerical analyses. Nowadays, fiber reinforced polymer (FRP) layers and steel elements are extensively utilized as appropriate techniques for enhancing the performance of concrete structures [1–3]. A state-of-the-art review on the FRP-strengthened reinforced concrete structures has been provided by Siddika et al. [4], which mainly focuses on their performances, modelling, failure mechanisms, challenges as well as opportunities.

Literature survey indicates that considerable research has been performed to evaluate the behavior of strengthened RC shear walls. In the following, some of these studies are addressed. Triantafillou [5] carried out an analytical as well as experimental investigation to examine the effects of FRP composites as a strengthening material on the ductility and strength of concrete structures. Lombard et al. [6] strengthened RC shear walls using unidirectional carbon fiber reinforced polymer (CFRP) laminates on both faces. The results demonstrated that the walls experienced higher values of the ultimate load and ductility. Ghobarah & Khalil [7] retrofitted RC shear walls implementing two bidirectional CFRP layers on the web of wall in addition to three unidirectional CFRP layers on the boundary elements. They used 45degree carbon fibers to postpone the shear failure of RC walls. The experimental results exhibited that the rehabilitation on schemes led to delay in the premature occurrence of failure in RC walls, and significantly enhanced the load bearing capacity. Altin et al. [8] studied the hysteresis behavior of deficient RC walls strengthened by CFRP layers under the applied lateral loading. They observed that the use of CFRP composites considerably improved the cyclic behavior of the RC walls. Qazi et al. [9] studied the seismic response of RC short shear walls strengthened

using partial CFRP layers. In this regard, strengthened walls with two different configurations and unidirectional CFRP composites were simulated under cyclic loading. The results indicated the satisfactory performance of strengthened RC walls in reference to the shear strength and deformability.

Although most of the researchers experimentally have investigated the efficiency of the strengthening methods on RC shear walls, numerous numerical analyses have been carried out in accordance with improvements made in the software applicability.

Vojdan and Aghayari [10] numerically investigated the seismic behavior of RC shear walls with opening retrofitted by FRP composites. They have retrofitted RC shear walls with different configurations of FRP sheets in ABAQUS software. Their results revealed that the applied FRP schemes increased the ultimate bearing strength, ductility, and behavior factor of strengthened walls. Husain et al. [11] developed a 3D nonlinear FE model to simulate the response of RC shear walls strengthened by CFRP composites under the monotonic loading. The results demonstrated that CFRP layers prevented premature failure of RC walls and decreased the stress concentration at the vicinity of opening. Hence, the failure occurred at higher values of the lateral load and ductility.

Despite the fact that there is a wealth of experimental and numerical studies performed to investigate the effects of attaching FRP composites in strengthening of RC shear walls, there are a few papers mainly concentrated on the applicability of using steel elements in the retrofitting of RC shear walls. Generally, it is easier and may be less expensive to apply FRP layers on shear walls, than steel strips or plates. It is required to compare these two techniques and determine the level of improvement in behavior by each approach.

As one of the primary contributions to this subject, Aviles et al. [12] wrapped critical sections of RC columns with thin steel elements to evaluate enhancement in shear strength and ductility. The RC columns were strengthened with four types of steel plates and subjected to cyclic lateral loading. The results showed that the strengthening of RC concrete columns altered the failure pattern at ultimate load. Furthermore, the results exhibited that if steel plates are combined with anchor bolts, the ductility and strength will be noticeably increased. Elnashai and Pinho [13] implemented steel elements in different configurations to improve the ductility, stiffness, and ultimate load capacity of RC walls. Taghdi et al. [14] conducted retrofitting by adding two vertical steel strips on each side of low-rise and non-ductile RC shear walls, which resulted in 50 % increase in the bearing capacity and changing the failure pattern

to shear sliding. Christidis et al. [15] examined the performance of non-conforming RC shear walls through applying various configurations of steel straps as well as steel angles to improve response parameters. To this end, five shear walls - one control wall and four strengthened walls- with slenderness ratio approximately equal to 2.0, were designed and tested under displacement control cyclic loading. All four strengthened RC walls restrained the occurrence of longitudinal reinforcement buckling in the compression zone along with preventing crack propagation in the wall surface. Limited numerical evaluation of shear walls strengthened by steel elements have been reported. Kheyroddin et al. utilized steel jackets at both ends in lieu of boundary elements in squat RC shear walls and the effectiveness of this strengthening method was investigated in terms of ductility and ultimate load capacity [16]. Zhou et al. [17] presented a nonlinear 3D finite element model to examine the cyclic performance of steel plate RC shear walls. In addition, the effect of influential parameters such as shear span ratio, steel plate ratio, and concrete strength has been scrutinized on the shear capacity of composite RC shear walls.

According to the above-mentioned, further analyses are required to numerically evaluate and compare the seismic response of strengthening methods implemented for RC shear walls. In order to improve the seismic performance of RC shear walls, for each strengthening method, new schemes require to be considered alongside those examined in the previous studies. Furthermore, it is of importance to find out the failure mechanisms of strengthened RC walls due to the proposed strengthening configurations. With the aim to comprehensively compare the seismic behavior of strengthened RC walls, not only the bearing capacity, but also the variation of different parameters including stiffness, energy dissipation, and ductility needs to be investigated due to the proposed configurations of strengthening techniques.

In this paper, nonlinear numerical simulations are carried out using ABAQUS [18], which is a conventional finite element (FE) analysis software. The RC walls are retrofitted by different schemes of CFRP composites and steel elements. In order to evaluate the response of strengthened walls under cyclic loading, parameters such as ductility, stiffness and energy absorption are determined. At the end, the behavior of CFRP composites strengthening approach is compared with that of steel elements.

2. Finite element simulation

The nonlinear analyses were accomplished by finite element program, ABAQUS version 6.18 to investigate the seismic response of strengthened RC shear walls. Extensive mesh studies

were carried out to identify appropriate mesh properties for all simulations. The FE simulations were desirable in terms of the running duration in addition to precision of the results. The results of the mesh sensitivity studies demonstrated that assigning element size of 8 and 12 cm for concrete materials and reinforcements were reasonable, respectively. Moreover, in order to preclude penetration of the interfaces, "Hard contact" was assumed for simulating the interaction between wall segments (foundation, RC wall, and loading beam).

In the following, FE modeling of strengthened RC shear walls is presented. The material characteristics are defined and introduced in distinct sub-sections to incorporate in the simulations. Fig. 1 depicts a schematic view of mesh pattern, steel reinforcements arrangements, and support condition of RC shear walls.

2.1. Concrete

Consideration of the nonlinear behavior of concrete materials is of particular importance in the modeling of RC structures. Toward this end, the Concrete Damage Plasticity (CDP) model was used for modeling of RC shear walls in FE software. In CDP model, several parameters such as the dilation angle, eccentricity, and viscosity are required. The values of these parameters are presented in Table 1. Furthermore, an eight-node, three transitional degrees of freedom with reduced integration (C3D8R) element was applied for the simulation of concrete materials.

2.1.1. Compressive behavior

Kent and Park model [19] was used to simulate the compressive characteristics of concrete (Fig. 2). The ascending part of the stress-strain curve is parabolic and follows a linear descending part up to $0.2\sigma_{cu}$, and then after, in region C-D, stress values remain constant.

For accounting geometric nonlinearity in the CDP model, the values of engineering stress and strain in both compression and tension regions were modified to the corresponding true values based on the following equations:

$$\sigma_{True} = \sigma_{Eng}(1+\varepsilon_{Eng}) \quad (1)$$

$$\varepsilon_{True} = Ln^{(1+\varepsilon_{Eng})} \quad (2)$$

In addition, in order to consider the effects of concrete crushing, softening coefficient (d_c) is defined as a damage parameter in the compressive region of concrete, which can be calculated based on the following formulation [20]:

$$d_c = 1 - \frac{\sigma_c}{\sigma_{cu}} \tag{3}$$

where σ_c and σ_{cu} stand for compressive stress in the post-peak region and the ultimate compressive stress of concrete, respectively. According to Eq. (3), the values of damage parameter are increased due to the decrease of compressive stress in the damage zone that results in stiffness degradation, which varies from 0 (undamaged concrete) to 1 (totally damaged concrete). In the FE analysis, the equations 4 to 6 are used to obtain the relation between different variables, including the plastic strain, compressive strength, and damage parameters of concrete material.

$$\varepsilon_c^{in,h} = \varepsilon_c - \frac{\sigma_c}{E} \tag{4}$$

$$\varepsilon_c^{pl,h} = \varepsilon_c - \frac{\sigma_c}{E}\left(\frac{1}{1-d_c}\right) \tag{5}$$

$$\varepsilon_c^{pl,h} = \varepsilon_c^{in,h} - \frac{\sigma_c}{E}\left(\frac{d_c}{1-d_c}\right) \tag{6}$$

in which $\varepsilon_c^{in,h}$, $\varepsilon_c^{pl,h}$ and E denote the inelastic strain, plastic strain, and concrete modulus of elasticity, respectively.

2.1.2 Tensile behavior

For simulating the brittle behavior of concrete materials, the recommended model of Nayal and Rasheed [21] was considered. As shown in Fig. 3, for the sake of eliminating computational errors induced by a sudden drop in the value of ultimate stress, the modified model of Wahalathantri et al. [22] was implemented. It is of interest to note that this model considers the effect of tension stiffening in the simulation of concrete properties. In the following, the value of tensile damage parameter (d_t) is determined based on Eq. (7):

$$d_t = 1 - \frac{\sigma_t}{\sigma_{tu}} \tag{7}$$

where σ_t and σ_{tu} denote the tensile stress in the post-peak region and the ultimate tensile stress of concrete material, respectively. Based on the above-mentioned equation, it can be observed that the concrete damage parameters represent the degradation of elastic stiffness in the tensile region. The governing stress-strain formulations under the uniaxial tensile loading are as follows:

$$\varepsilon_t^{ck,h} = \varepsilon_t - \frac{\sigma_t}{E} \tag{8}$$

$$\varepsilon_t^{pl,h} = \varepsilon_t - \frac{\sigma_t}{E}\left(\frac{1}{1-d_t}\right) \tag{9}$$

$$\varepsilon_t^{pl,h} = \varepsilon_t^{ck,h} - \frac{\sigma_t}{E}\left(\frac{d_t}{1-d_t}\right) \tag{10}$$

wherein $\varepsilon_t^{ck,h}$ and $\varepsilon_t^{pl,h}$ are the values of crack and plastic strains, respectively. Table 2 summarizes the values of calculated parameters involved in the numerical simulation of concrete material.

2.2. Steel reinforcements

Steel reinforcements consist of longitudinal and transverse steel rebars simulated with three-dimensional, two nodes truss element (T2D3) in the FE analysis. In the interaction module, steel reinforcements were embedded in concrete materials. The elastic-plastic behavior was assumed for the property of steel materials (reinforcements and elements).

2.3. CFRP and epoxy model

Carbon fiber reinforced polymer (CFRP) in different arrangements was used to strengthen concrete RC shear walls. The simulation of CFRP laminates was conducted based on a four-node shell element with reduced integration (S4R). The cohesive behavior was considered on the basis of epoxy resin and concrete characteristics, which examines the occurrence of CFRP separation from the concrete interface.

2.4. Steel elements

Steel elements in different configurations were utilized for retrofitting of RC shear walls. As the thickness of steel elements is small in comparison with the wall thickness, the S4R element was used to model steel elements in the simulations. Mechanical properties of steel reinforcements, CFRP layers, epoxy resin, and steel elements are presented in Table 3.

3. Verification of FE models

In order to evaluate the validation of numerical simulations investigated in this paper, the experimental results of the previous studies were considered. To verify shear walls strengthened by steel elements models, one of the shear walls tested by Christidis et al. [15] was simulated in the FE software. The wall's aspect ratio was approximately equal to 2.0, and

steel elements were wrapped along the shear wall's height to improve the shear capacity. Verification of the CFRP layers conducted through one of the models examined by Qazi et al. [9]. In this model, the CFRP strips were bonded in both horizontal and vertical orientations, which were parallel to steel reinforcements. The load displacement curves of the performed numerical simulations are presented in Fig. 4. As can be seen from this figure, the accuracy of FE simulation is satisfactory in response prediction.

4. Model characteristics

The design of RC shear walls was carried out according to Eurocode [23,24]. The section of wall is rectangular with the length and thickness of 0.8 m, and 12.5 cm, respectively. The height of wall is considered to be 1.5 m for all models. The steel reinforcements consist of 10 mm diameter with 180 mm spacing for longitudinal and 8 mm diameter with 250 mm spacing for transverse rebar, which corresponds to reinforcement ratios equal to 0.78% and 0.37%, respectively. The foundation of all RC shear walls was reinforced using steel rebar of 14 mm diameter equally spaced at 180 mm and 8 mm stirrups at 24 cm spacing. Also, 4 cm was taken as clear cover for the foundation. All the steel reinforcements were embedded into the foundation, wall, and loading beam segments in order to ensure the monolithic behavior of the shear wall. Fig. 5 shows geometrical dimensions, reinforcements characteristics, and configurations of steel reinforcements of RC shear wall. It is to mention that, the control shear wall (CSW) was designed so that the flexural failure occurred due to the applied lateral loading. In this regard, steel elements and also CFRP as strengthening systems were utilized in different configurations to enhance the ductility and bearing capacity of RC walls.

All the simulations conducted under the action of displacement-control cyclic loading. The cyclic loading history consists of three cycles for each target drift in order to reach the expected failure of strengthened RC shear wall. As is shown in Fig. 6, the lateral displacement was applied at center of the loading beam with drift values of 0.1%, 0.2%, …., 1.5%. Furthermore, the loading beam was assumed to be rigid in order to uniformly transfer the applied loading into the strengthened RC shear wall.

4.1. CFRP arrangements

In order to address the effects of CFRP composites in the cyclic performance of strengthened RC shear walls, four different configurations were examined through nonlinear FE analysis. These configurations were selected according to the conventional strengthening techniques

used in the previous experimental studies [9,10] as well as the arrangements proposed by the authors. All of the schemes were modeled with both one layer and two layers of vertical-oriented CFRP laminates of 0.2 mm thickness which are introduced as follows:

(1) Totally covered on both sides of the shear wall with CFRP laminate (SSW-CF1);

(2) Coverage on both sides of the shear wall with 40 cm of CFRP at the top and bottom (SSW-CF2); (Fig. 7(a))

(3) Coverage on both sides of the shear wall using four 16 cm horizontal layers and two 16 cm vertical layers (SSW-CF3); (Fig. 7(b))

(4) Coverage on both sides of the shear wall using one 16 cm horizontal layer and three 16 cm vertical layers (SSW-CF4). (Fig. 7(c))

The schematic view of above-mentioned arrangements for SSW-CF2, SSW-CF3, and SSW-CF4 depicted in Fig. 7 (wall surface and CFRP layers are in blue and orange, respectively).

4.2. Steel elements arrangements

Four different schemes were defined for steel elements to strengthen the CSW. In all cases, the interface between steel elements and surface of the shear wall was simulated using tie interaction. The numerical models were created in accordance with the experimental specimens examined by Elnashai and Pinho [13], and Christidis et al. [15]. In the following, the arrangements of steel elements in RC shear walls are defined:

(1) Wrapped shear wall with nine equidistant 4 cm steel strips along the wall's height (SSW-ST1); (Fig. 8(a))

(2) Wrapped shear wall with nine equidistant 4 cm steel strips along the wall's height in addition to four 5 cm steel angles at all edges (SSW-ST2); (Fig. 8(b))

(3) Coverage on both sides of the shear wall with three 10 cm steel plates (SSW-ST3); (Fig. 8(c))

(4) Coverage on both sides of the shear wall using two steel plates with 25 cm width and 40 cm height at the bottom edges of the wall's length (SSW-ST4). (Fig. 8(d))

It is to mention that, for all cases, the thickness of steel elements is taken to be 0.5 mm. Fig. 8 (a-d) illustrates the configurations of steel elements utilized in the FE simulations.

5. Analysis results

In the following, seismic response of strengthening methods for retrofitting RC walls are examined and compared in terms of ductility, secant stiffness, dissipated energy obtained from load-displacement envelope curves, then, a number of failure patterns are demonstrated.

5.1. Load-displacement

The envelope of hysteresis curves for RC shear walls strengthened by CFRP laminates and steel elements are shown in Fig. 9 and Fig. 10, respectively. In these load-displacement curves, the failure occurrence was assumed so that the value of load in the descending region reached approximately 85% of the ultimate load.

In order to better compare the effect of strengthening methods on the ultimate load capacity of RC shear walls, the best arrangement of each method is demonstrated in Fig. 11. It can be revealed that in both cases, the seismic behavior of the strengthened RC shear walls has been improved.

5.2. Ductility

Displacement ductility has been commonly adopted as an appropriate criterion due to its transparent correlation with the nonlinear hysteretic behavior [25]. For obtaining the ductility of strengthened RC shear walls, the bilinear ideal elastic-plastic curve was considered. In this study, the method based on balanced energy (MBBE) was implemented, in which area under the load-displacement curve and ideal curve must be identical (Fig. 12). The ratio between the ultimate displacement (Δ_u) to yield displacement (Δ_y) is defined as ductility, which represents the capability of strengthened RC shear walls to sustain nonlinear deformations:

$$\mu = \frac{\Delta_u}{\Delta_y} \tag{11}$$

In accordance with Eq. (11) and the values of ultimate displacement as well as yield displacement obtained from the idealized bilinear elastic-plastic curves, corresponding displacement ductility of strengthened RC shear walls are calculated and listed in Table 4.

5.3. Secant stiffness

The secant stiffness is an index that examines the degradation of stiffness induced by nonlinear deformations in structural elements due to the excitation of cyclic loading. To this

end, this index is defined as the ratio between the load and corresponding displacement at each cycle of loading, which can be determined based on the following equation [26]:

$$K_i = \frac{|F_i|+|-F_i|}{|X_i|+|-X_i|} \tag{12}$$

in which i denotes the number of loading cycle, F_i and X_i are the maximum load and displacement corresponding to the maximum load in the i-th loading cycle, respectively. The stiffness degradation variations of strengthened RC shear walls are illustrated in Fig. 13. According to the results obtained from the stiffness degradation curves, for all strengthened RC shear walls, the values of initial stiffness were increased. Also, a decrease in stiffness values was generally observed after each cycle of loading that mainly induced by concrete cracking, concrete crushing, and yielding of steel reinforcements. The slope of stiffness was steeper at the onset of Stiffness-Drift curves before cracks propagation on the surface of concrete. Furthermore, the effect of number of CFRP layers on the stiffness of strengthened RC walls was not meaningful. The highest initial stiffness was also seen for the configurations of SSW-ST2 and SSW-ST3, which increased the initial stiffness up to twice the CSW.

5.4. Dissipated energy

The dissipated energy in each cycle was measured by calculating the area enclosed by each cycle of hysteresis load-displacement curves. The variation of dissipated energy with respect to the values of applied drift are presented in Fig. 14.

5.5. Failure patterns

By conducting an observation on the variation of damage parameter, maximum principal plastic strain, and stress contours, the failure patterns of simulated RC shear walls are determined and presented in Fig. 15 (a-d). According to this figure, the failure patterns can be listed as follow: (1) crack propagation on the wall, (2) yielding of reinforcements, (3) delamination of CFRP laminates bonded to concrete, (4) concrete bulging.

6. Discussion

In order to investigate the efficiency of the proposed strengthening methods, the values of influential response parameters including the ultimate load capacity, maximum displacement, yielding displacement, ductility, as well as the energy absorption were obtained and summarized in Table 4.

As shown in this table, almost all of the strengthened walls achieved higher ultimate load capacity, energy absorption, and ductility in comparison to the CSW. As previously mentioned, the CSW was designed so that flexure was the dominant failure mechanism in the seismic loading. It was observed that concrete spalling at the bottom edges of the wall followed by buckling as well as fracture of rebars resulted in the failure of CSW. (see Fig. 15(a-b)) [15]. From Fig. 15(a), it can also be seen that a continuous horizontal crack has been propagated near the wall foundation joint. In fact, the reinforcement ratio was not sufficient enough to prevent the above-mentioned failure modes of control RC wall. Thus, an enhancement in the seismic performance of strengthened RC walls can be attributed to the delay of premature failure in the concrete and steel rebars.

By observing the values of Table 4, it can be seen that using CFRP laminates and steel elements improved the ultimate load capacity by 34 % and 70 %, when compared with CSW, which corresponds to SSW-CF3-2L and SSW-ST2, respectively. In the CFRP-strengthened RC walls, an increase in the ultimate load capacity can be attributed to the load contribution of CFRP laminates as well as the prevention of crack propagation. Indeed, the CFRP layers can postpone the occurrence of premature failure in the strengthened walls. Except for SSW-CF2-2L, the ultimate load was slightly increased with an increase in the number of CFRP layers. It is worth mentioning that for SSW-CF2-2L, the applied strengthening arrangement modified the failure mechanism from flexure to shear. This characteristic can be attributed to the confinement effects induced by increasing the number of CFRP layers, which results in reduction of the effective length of the RC shear wall. In all CFRP-strengthened RC walls, except SSW-CF2-2L, the failure occurred after debonding of CFRP laminates from wall surface (Fig. 15(c)). In SSW-ST1 and SSW-ST2, an improvement in the bearing capacity was observed due to the prevention of the premature buckling of steel rebars. In this regard, the unsupported bar length is expressed as an influential factor for buckling behavior of steel bars, which has been decreased in SSW-ST1 due to the confining effects of the steel straps. Almost no buckling was observed in the steel bars of SSW-ST2 owing to the presence of steel angle. In contrary to SSW-ST2, no noticeable change was detected in the initial stiffness of SSW-ST1, since the flexural cracks are still being developed at both corners of the wall. In SSW-ST3 and SSW-ST4, the initial stiffness has been increased due to the prevention of crack propagation at the corners of the walls. Furthermore, the occurrence of premature concrete crushing as well as the buckling of rebars was restrained at the corners of walls which can be associated with the confinement effects provided by means of steel plates. Particularly, In

SSW-ST2, SSW-ST3, and SSW-ST4, the occurrence of uplift at the wall-foundation interface was observed as one of the major failure mechanisms (Fig. 15(d)), which provides higher load bearing capacity. For example, in SSW-ST2 configuration with the highest peak load, the foundation was involved in the failure mechanism owing to the sturdy connection of steel straps, angles, and concrete wall which approximately acts similar to an anchor attaching RC wall to the foundation. Therefore, it is expected that the peak load in SSW-ST2 to be noticeably more than that of CSW. As shown in Fig. 15(d), steel plates and steel corners shifted the crack propagation from covered regions to uncovered regions [12]. Almost all the proposed strengthening arrangements enhanced the ultimate displacement of RC shear wall. It also can be observed from Table 4 that SSW-CF3-2L and SSW-ST3 configurations indicated better performance than other configurations so that they increased the ultimate displacement by 25%, when compared to CSW.

All strengthened RC shear walls except for SSW-CF2-2L, SSW-CF3-2l, SSW-CF4-2L, and SSW-ST1 exhibited an increase in the value of displacement ductility in comparison to CSW. It is noteworthy to mention that for all RC walls strengthened with two layers of CFRP laminates, lower displacement ductility was observed compared to one layer of CFRP. This observation is due to the fact that the shear failure mechanism governs the behavior of strengthened RC walls. Retrofitting RC shear walls with steel elements indicated better performance in terms of the ultimate displacement and ductility in comparison to the previously described method.

By calculating the area under the load-displacement envelope curves, energy absorption capability of the proposed strengthening methods was investigated. The values of energy absorption were summarized in Table 4. The energy absorption increased significantly for all models except SSW-CF4-1L. Furthermore, the most increase in the value of energy absorption was observed for SSW-ST2, which was twice as large as that of CSW.

The numerical results of FE simulations suggest that retrofitting of RC shear walls using CFRP laminates and steel elements can improve the capability of these structural elements to sustain nonlinear deformations under seismic loading.

7. Conclusion

The present study is an attempt to examine the seismic performance of RC shear walls strengthened with CFRP composites and steel elements. Four different configurations of CFRP composites (four in one layer and four in two layers) and four different arrangements of steel

elements were considered and simulated using finite element methodology under the lateral cyclic loading. Based on the conducted investigations, the following conclusions can be drawn:

- A finite element simulation has been established to evaluate the cyclic response of strengthened RC shear walls, and the qualification of the procedure was ascertained through previous experimental research.
- Utilizing both CFRP laminates and steel elements remarkably increased the ultimate load capacity. In comparison to CFRP laminates, steel elements are more efficient in increasing the ultimate load. In SSW-ST2 and SSW-ST3, the occurrence of uplift at the wall-foundation interface was observed as the major failure mechanism which provided higher load bearing capacity. For example, SSW-ST2 enhanced the ultimate load capacity about 70%. Also, a slight variation was observed in the values of ultimate load with an increase in the number of CFRP layers.
- The ultimate displacement of strengthened RC walls generally increased in comparison with the control shear wall (CSW), in which SSW-CF3-2L and SSW-ST3 are more advantageous by an increase of 25%.
- The displacement ductility ranges from 2.51 (SSW-CF2-1L) to 3.28 (SSW-ST3). The effect of proposed strengthening methods on the displacement ductility was not significant, except for SSW-ST2, SSW-ST3. The values of ductility reduced by increasing the number of CFRP layer due to the change in the failure mechanism from flexure to shear. The performance of steel elements arrangements in increasing the displacement ductility was more appropriate as compared to using CFRP laminates.
- The slope of stiffness degradation was decreased by an increase in the values of lateral displacement due to the nonlinear behavior of materials. The initial stiffness in the first cycle of lateral loading ranges from 25 to 48 (kN/mm). SSW-ST2 and SSW-ST3 considerably augmented the initial stiffness up to twice the CSW due to more confinement provided by the proposed strengthening configurations, whereas an increase in the initial stiffness is not meaningful for other arrangements.
- The values of energy absorption for strengthened RC shear walls indicated a significant increase, which implied that the proposed strengthening methods were desirable in seismic events. As concluded from the numerical outcomes, SSW-CF3-2L, SSW-ST2, and SSW-ST3 had the superior performance in terms of seismic responses evaluated in this research. In the sense that, the above-mentioned configurations are more

advantageous in the enhancement of energy absorption, ultimate load capacity, as well as ultimate displacement.

- The failure mechanism of RC shear walls strengthened with CFRP laminates was observed due to concrete crushing, yielding of steel reinforcements in the wall's edges, and delamination of CFRP layers from concrete surface. For another strengthening method, the main failure mechanism of RC shear walls was found to be the foundation bulging as well as the yielding of steel reinforcements at the wall-foundation interface.

Acknowledgments

The authors highly appreciate the supports provided by the Center of Excellence in Composite Structures and Seismic Strengthening (CECSSS) at Sharif University of Technology.

References

1. Bakis, C. E., Bank, L. C., Brown, V. L., Cosenza, E., Davalos, J. F., Lesko, J. J., Machida, A., Rizkalla, S. H., and Triantafillou, T. C., "Fiber-reinforced polymer composites for construction - State-of-the-art review", *Journal of Composites for Construction*, **6**(2), pp. 73–87 (2002).

2. Marini, A. and Meda, A., "Retrofitting of R/C shear walls by means of high performance jackets", *Engineering Structures*, **31**(12), pp. 3059–3064 (2009).

3. Mostofinejad, D. and Mohammadi Anaei, M., "Effect of confining of boundary elements of slender RC shear wall by FRP composites and stirrups", *Engineering Structures*, **41**, pp. 1–13 (2012).

4. Siddika, A., Al Mamun, M. A., Ferdous, W., and Alyousef, R., "Performances, challenges and opportunities in strengthening reinforced concrete structures by using FRPs-A state-of-the-art review", *Engineering Failure Analysis*, p. 104480 (2020).

5. Triantafillou, T. C., "Strengthening of structures with advanced FRPs", *Progress in Structural Engineering and Materials*, **1**(2), pp. 126–134 (1998).

6. Lombard, J., Lau, D. T., Humar, J. L., Foo, S., and Cheung, M. S., "Seismic strengthening and repair of reinforced concrete shear walls", *Proc., 12th World Conf. on Earthquake Engineering*, pp. 1–8 (2000).

7. Ghobarah, A. and Khalil, A. A., "Seismic rehabilitation of reinforced concrete walls using fibre composites", *Proceedings of the 13th World Conference on Earthquake Engineering, Vancouver, BC, Canada, August*, pp. 1–6 (2004).

8. Altin, S., Anil, Ö., Kopraman, Y., and Kara, M. E., "Hysteretic behavior of RC shear walls strengthened with CFRP strips", *Composites Part B: Engineering*, **44**(1), pp. 321–329 (2013).

9. Qazi, S., Michel, L., and Ferrier, E., "Seismic behaviour of RC short shear wall strengthened with externally bonded CFRP strips", *Composite Structures*, **211**, pp. 390–400 (2019).

10. Mohammadi Vojdan, B. and Aghayari, R., "Investigating the seismic behavior of RC shear walls with openings strengthened with FRP sheets using different schemes", *Scientia Iranica*, **24**(4), pp. 1855–1865 (2017).

11. Husain, M., Eisa, A. S., and Hegazy, M. M., "Strengthening of reinforced concrete shear walls with openings using carbon fiber-reinforced polymers", *International Journal of Advanced Structural Engineering*, **11**(2), pp. 129–150 (2019).

12. Aviles, N. B., Maruyama, K., and Rojas, L. E., "Improving strength and ductility by using steel plate

wrapping", *Proceeding of the 11th World Conference on Earthquake Engineering, Paper No* (1996).

13. Elnashai, A. S. and Pinho, R., "Repair and retrofitting of RC walls using selective techniques", *Journal of Earthquake Engineering*, **2**(04), pp. 525–568 (1998).

14. Taghdi, M., Bruneau, M., and Saatcioglu, M., "Seismic retrofitting of low-rise masonry and concrete walls using steel strips", *Journal of Structural Engineering*, **126**(9), pp. 1017–1025 (2000).

15. Christidis, K. I., Vougioukas, E., and Trezos, K. G., "Strengthening of non-conforming RC shear walls using different steel configurations", *Engineering Structures*, **124**, pp. 258–268 (2016).

16. Kheyroddin, A. and Naderpour, H., "Nonlinear finite element analysis of composite RC shear walls", *Iranian Journal of Science and Technology*, **32**(B2), p. 79 (2008).

17. Zhou, Z., Qian, J., and Huang, W., "Shear strength of steel plate reinforced concrete shear wall", *Advances in Structural Engineering* (2020).

18. SIMULIA, "ABAQUS/Standard Version 6.18 Analysis User's Manual" (2018).

19. Kent, D. C. and Park, R., "Flexural members with confined concrete", *Journal of the Structural Division* (1971).

20. Hafezolghorani, M., Hejazi, F., Vaghei, R., Jaafar, M. S. Bin, and Karimzade, K., "Simplified damage plasticity model for concrete", *Structural Engineering International*, **27**(1), pp. 68–78 (2017).

21. Nayal, R. and Rasheed, H. A., "Tension stiffening model for concrete beams reinforced with steel and FRP bars", *Journal of Materials in Civil Engineering*, **18**(6), pp. 831–841 (2006).

22. Wahalathantri, B. L., Thambiratnam, D. P., Chan, T. H. T., and Fawzia, S., "A material model for flexural crack simulation in reinforced concrete elements using ABAQUS", *Proceedings of the First International Conference on Engineering, Designing and Developing the Built Environment for Sustainable Wellbeing*, Queensland University of Technology, pp. 260–264 (2011).

23. Dumova-Jovanoska, Elena, " Drafting of Macedonian NDPs for EN 1998 - Design of structures for earthquake resistance - Part 3: Assessment and retrofitting of buildings", *15th World Conference on Earthquake Engineering (15WCEE)* (2012).

24. EN, C. E. N., "3 Eurocode 8: design of structures for earthquake resistance-part 3: assessment and retrofitting of buildings", *European Committee for Standardization, Brussels, Belgium* (2005).

25. Park, R., "Ductility evaluation from laboratory and analytical testing", *Proceedings of the 9th World Conference on Earthquake Engineering, Tokyo-Kyoto, Japan*, pp. 605–616 (1988).

26. Sullivan, T. J., Calvi, G. M., and Priestley, M. J. N., "Initial stiffness versus secant stiffness in displacement based design", *13th World Conference of Earthquake Engineering (WCEE)*, Citeseer (2004).

Biographies

Omid Habibi received the BSc and MSc degrees from Sharif University of Technology in 2017 and 2020, respectively, Tehran, Iran. He is currently working as a Research Assistant with Prof. Khaloo. His research interests are reinforced concrete structures, rehabilitation and retorting of structures, finite element analysis, seismic behavior of structures, and FRP composites. He is also a member of Iran's national elite foundation.

Alireza Khaloo received PhD from North Carolina State University. Since 1988, he has been in the Civil Engineering Department at Sharif University of Technology, where he is currently

a Distinguished Professor. Prof. Khaloo's research is related to the behavior of reinforced and prestressed concrete structures, seismic behavior of structures, advanced concrete technology, earthquake engineering, impact response of concrete structures, composite materials, and rehabilitation as well as strengthening various types of structures. He has contributed and been involved in major projects such as Milad Tower and Masjed Soleiman Dam. Moreover, He had the main role in conducting different retrofitting projects such as refineries, petrochemical platforms, and sophisticated structures.

Hatef Abdoos received the BSc and MSc degrees from Sharif University of Technology in 2012 and 2015, respectively. He is currently pursuing his PhD degree at Sharif University of Technology in Structural Engineering in the field of curved structures under supervision of Prof. Khaloo. His main research interests include analytical as well as experimental analysis of reinforced concrete members, finite element analysis, retrofitting/strengthening of structural members, FRP composites, and construction materials. He is also a member of Iran's national elite foundation and invited lecturer at Sharif University of technology from 2018.

Figures:

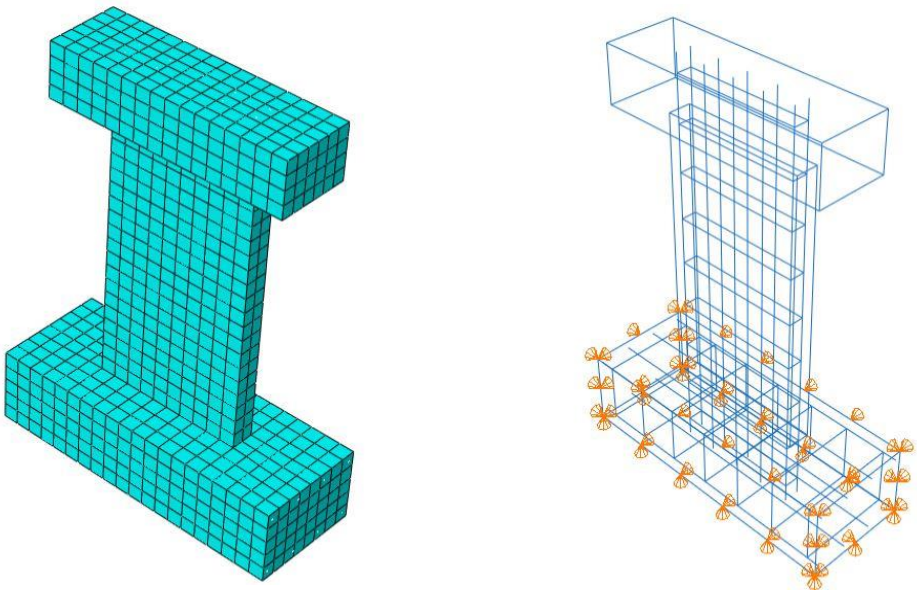

(a) (b)

Fig. 1. Schematic view of RC shear wall: (a) wall mesh pattern; (b) reinforcements arrangements and support condition.

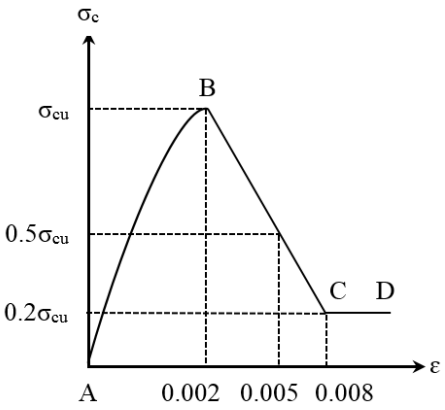

Fig. 2. Kent and Park Model for the compressive behavior of concrete [19].

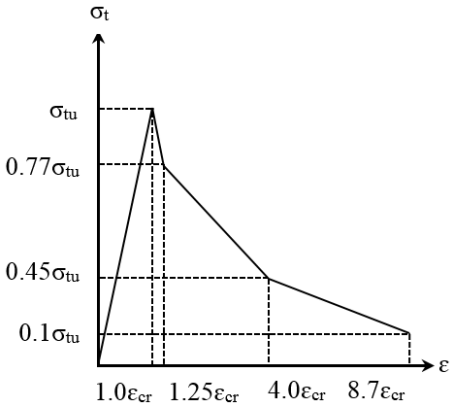

Fig. 3. Stress-strain curve, tension [Modified Nayal and Rasheed model].

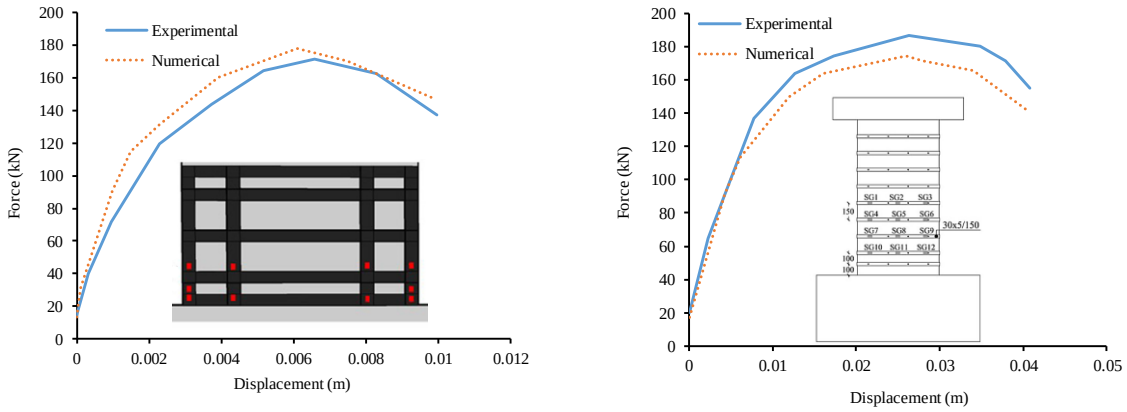

(a) (b)

Fig. 4. Load displacement curves from experimental and numerical analyses: (a) Steel elements; (b) CFRP composite.

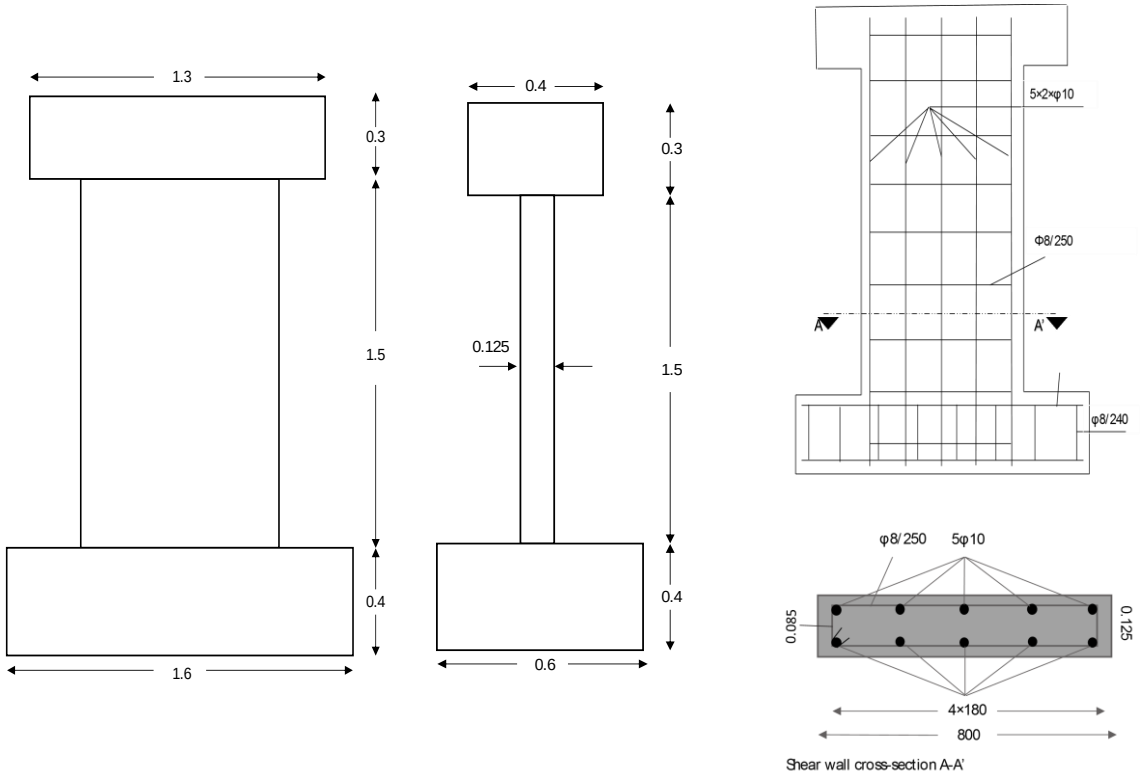

(a) (b)

Fig. 5. Geometrical dimensions and reinforced characteristics of the model: (a) geometrical dimensions; (b) characteristics and configuration of steel reinforcements.

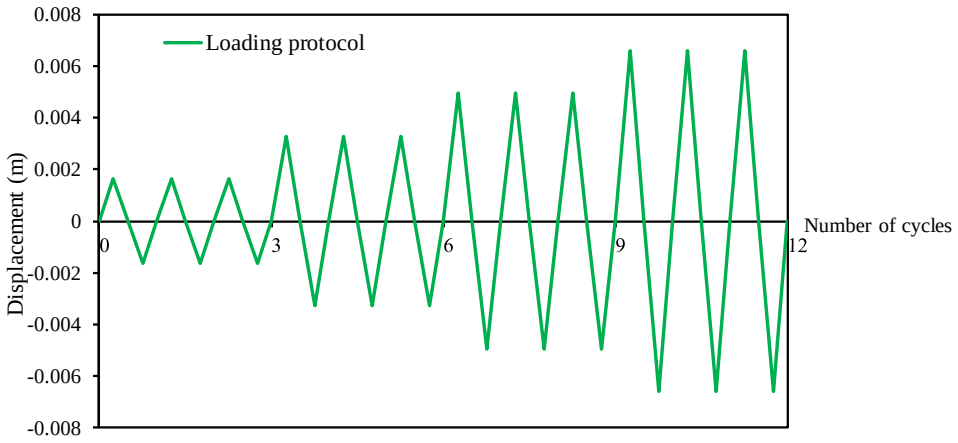

Fig. 6. Cyclic loading pattern.

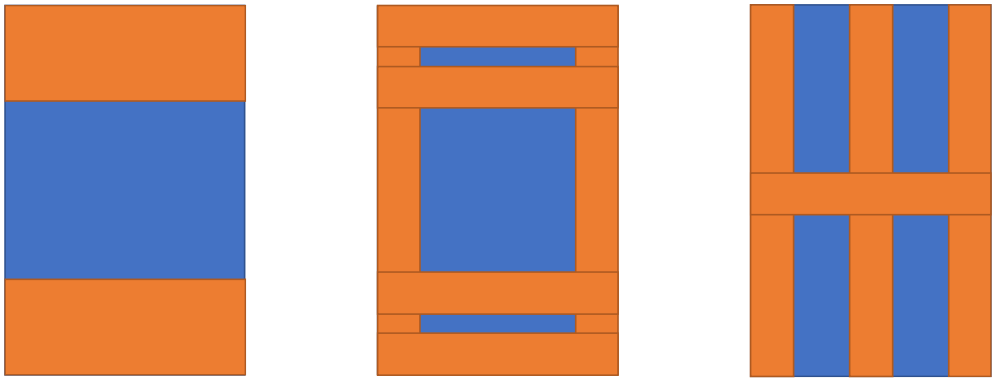

(a) (b) (c)

Fig. 7. CFRP composites models: (a) SSW-CF2; (b) SSW-CF3; (c) SSW-CF4.

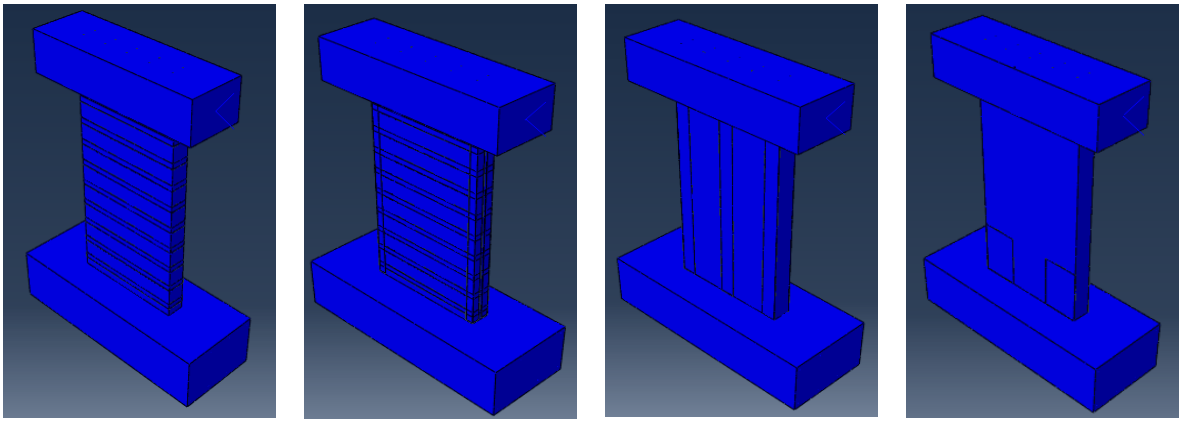

(a) (b) (c) (d)

Fig. 8. Steel elements configurations: (a) SSW-ST1; (b) SSW-ST2; (c) SSW-ST3; (d) SSW-ST4.

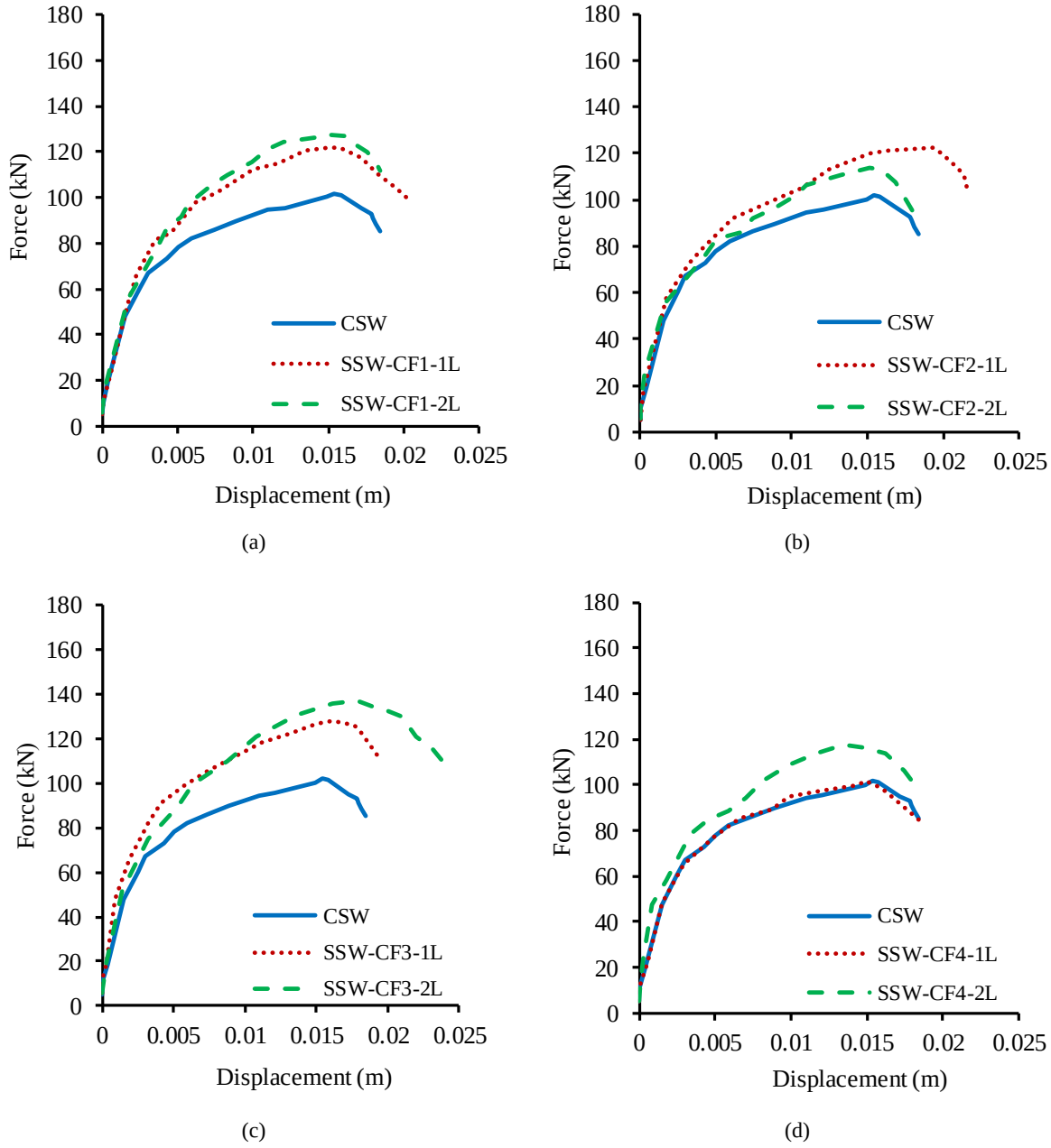

Fig. 9. Comparison of load-displacement curves for RC walls strengthened by CFRP schemes vs CSW: (a) SSW-CF1-1L, SSW-CF1-2L; (b) SSW-CF2-1L, SSW-CF2-2L; (c) SSW-CF3-1L, SSW-CF3-2L; (d) SSW-CF4-1L, SSW-CF4-2L.

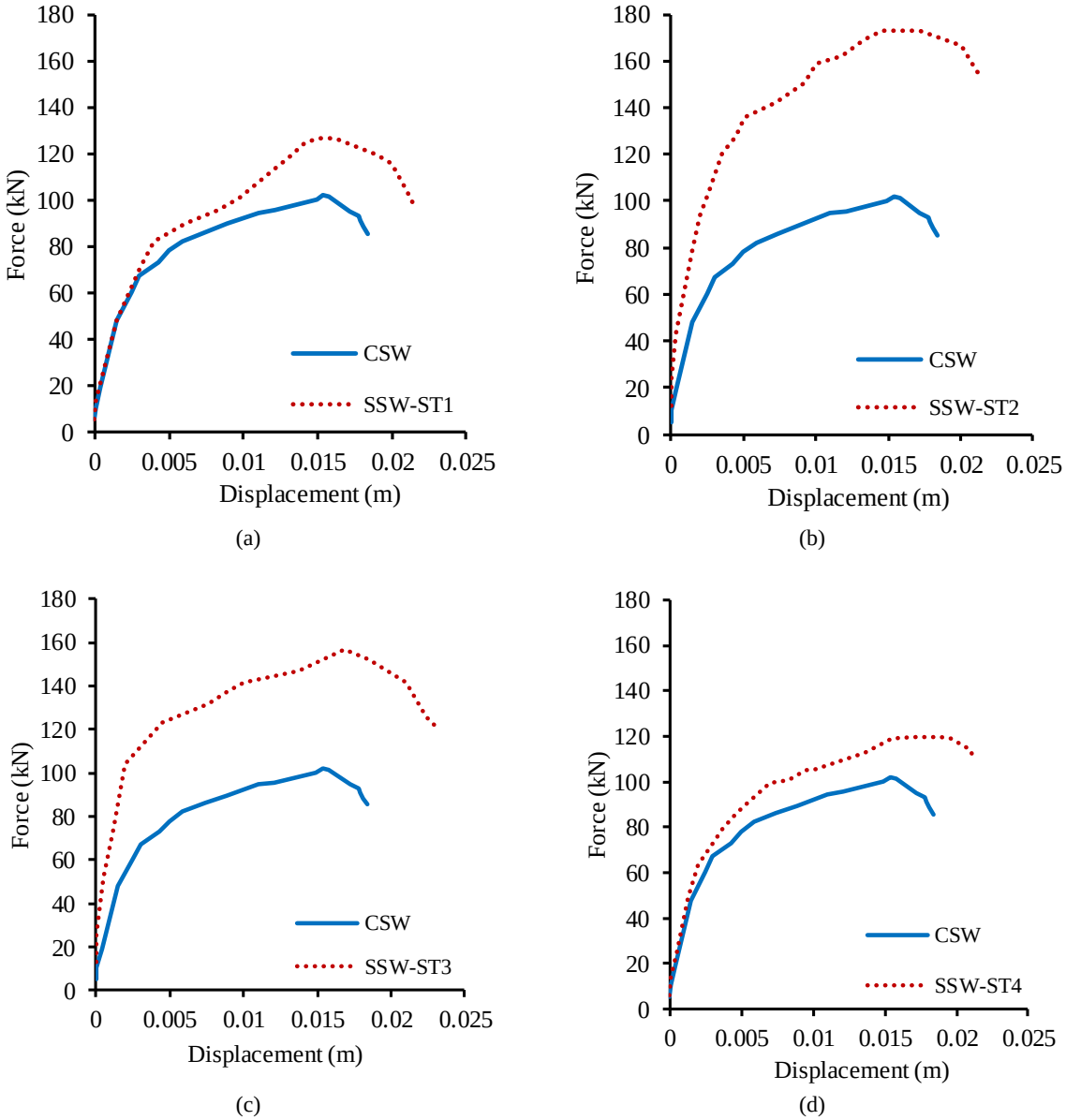

Fig. 10. Comparison of load-displacement curves for RC walls strengthened with steel elements vs CSW: (a) SSW-ST1; (b) SSW-ST2; (C) SSW-ST3; (d) SSW-ST4.

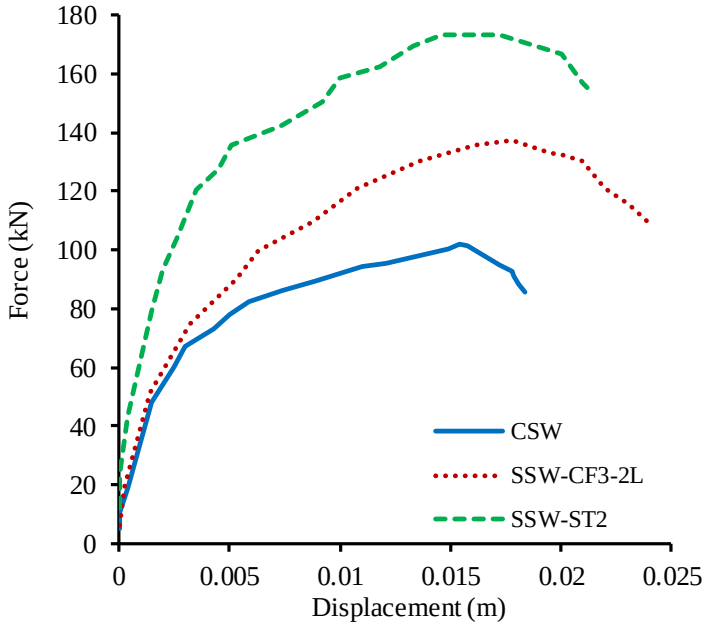

Fig. 11. Comparison of Load-displacement curves between SSW-CF3-2L, SSW-ST2 and CSW.

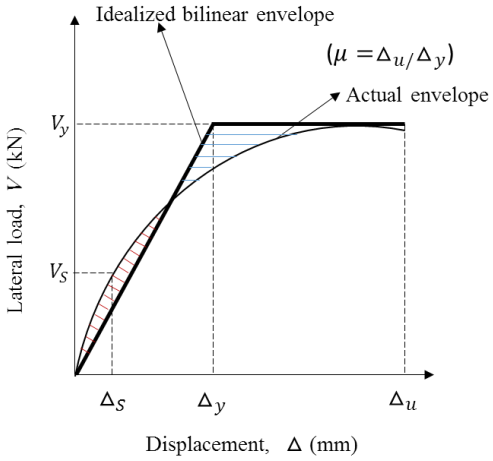

Fig. 12. Idealized bilinear envelope curve.

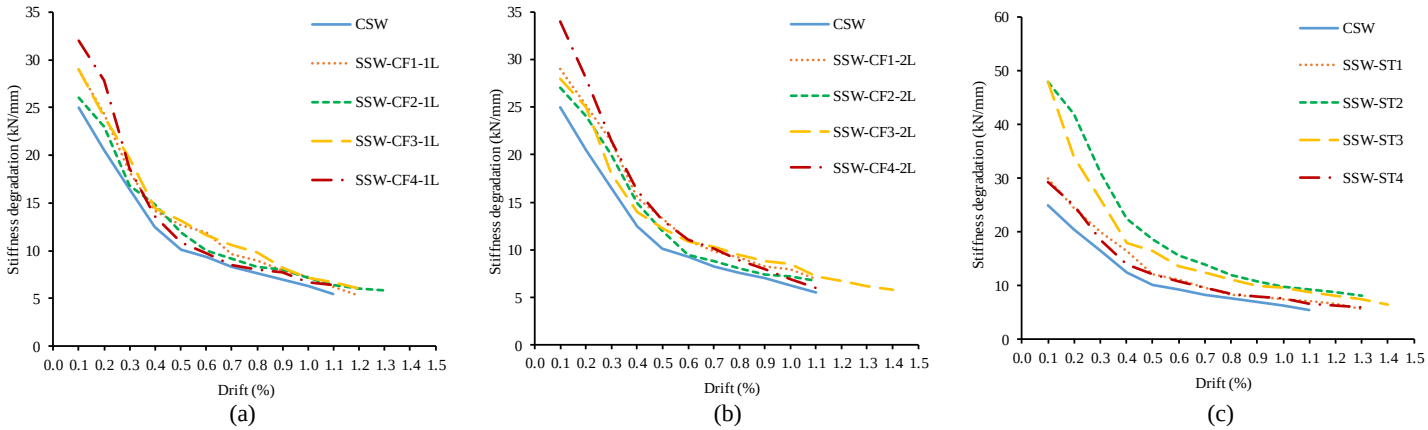

Fig. 13. Stiffness degradation in each implemented drift: (a) one layer CFRP composite; (b) two layers CFRP composite; (c) steel elements.

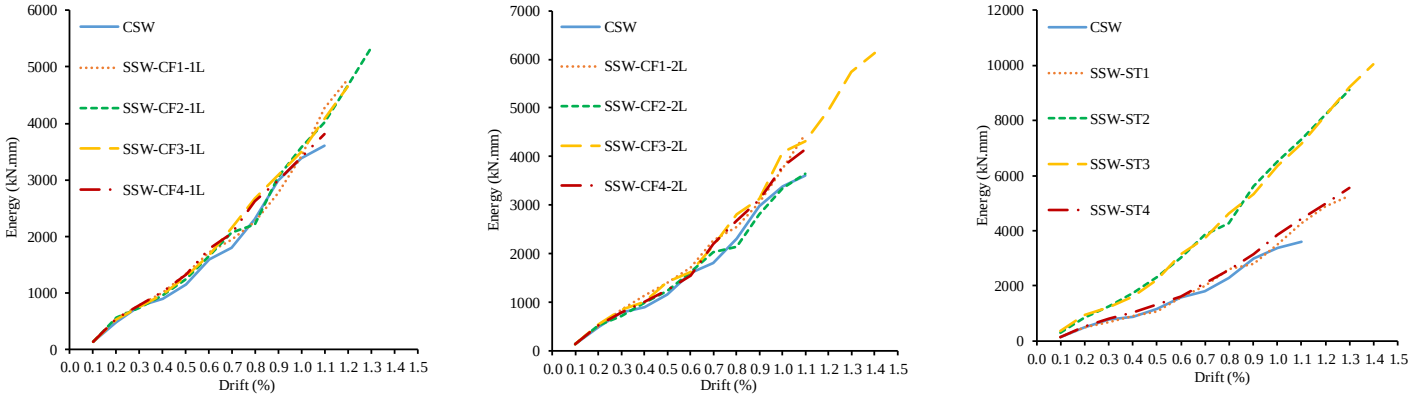

Fig. 14. Energy dissipation in the first cycle of each implemented drift: (a) one layer CFRP composite; (b) two layers CFRP composite; (c) steel elements.

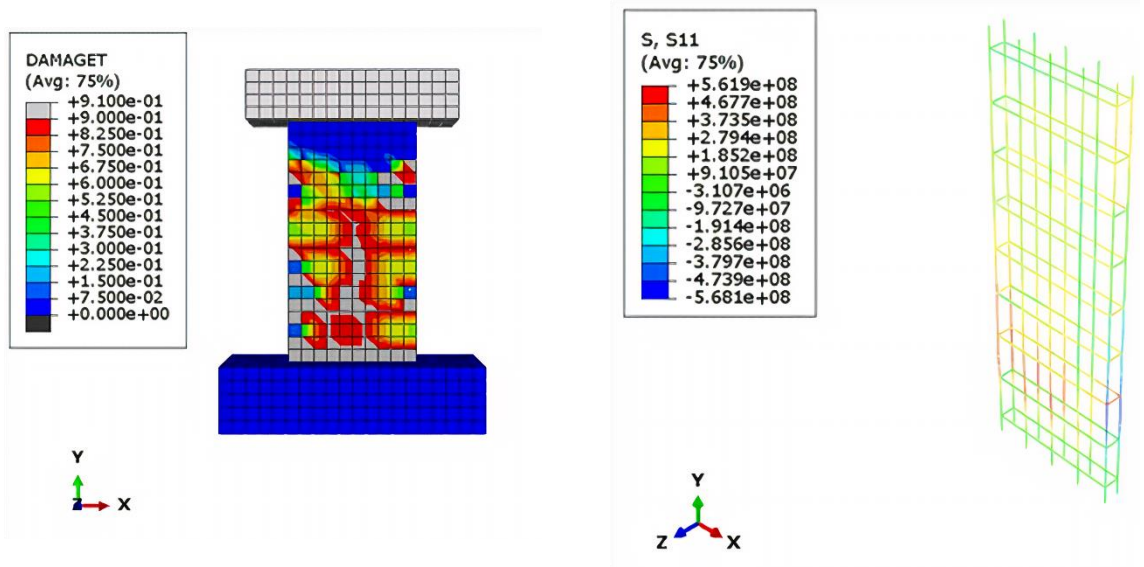

(a) (b)

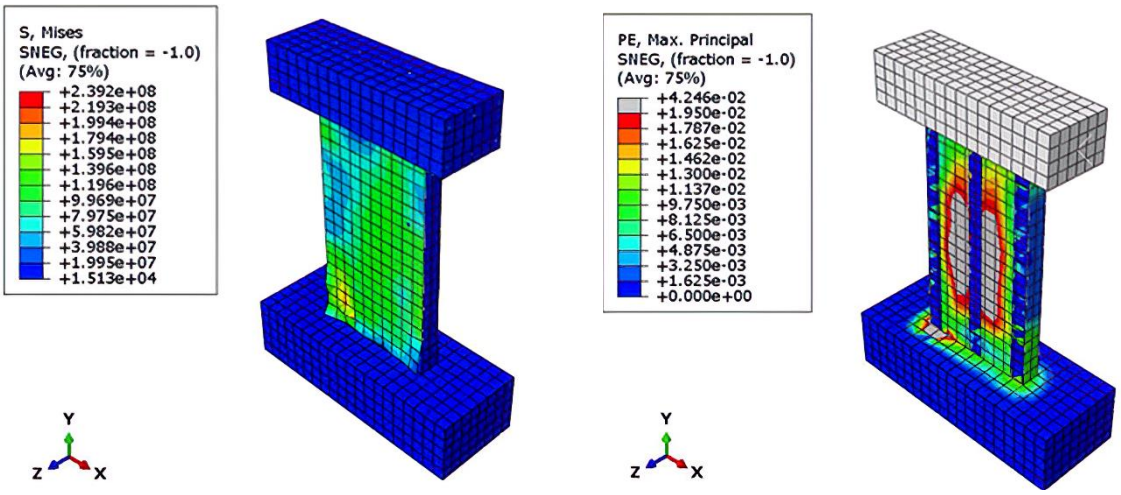

(c) (d)

Fig. 15. Failure patterns of simulated walls: (a) Crack propagation on the wall (SCW); (b) Yielding of longitudinal reinforments (SSW-ST1); (c) Delamination of CFRP laminates (SSW-CF1-2L); (d) Concrete bulging at the base level and crack propagation in un-retroffited regions.

Tables:

Table 1. Details of concrete parameters.

Dilation angle	Eccentricity	f_{b0}/f_{c0}	k	Viscosity parameter
30	0.1	1.16	0.67	0.001

Table 2. Concrete material properties.

Concrete compressive behavior		Concrete compression damage	
Stress (MPa)	Inelastic strain	Damage parameter	Inelastic strain
12.5	0	0	0
17.3	0.00013	0	0.00013
24.7	0.000761	0	0.000761
25.05	0.001	0	0.001
20.01	0.00219	0.196	0.00219
17.1	0.0036	0.316	0.0036
14.1	0.00393	0.436	0.00393
12.6	0.00436	0.496	0.00436
10.1	0.00548	0.596	0.00548
8.05	0.00637	0.68	0.00637
5.04	0.00772	0.798	0.00772
Concrete tensile behavior		Concrete tension damage	
Stress (MPa)	Crack strain	Damage parameter	Crack strain
2.5	0	0	0
1.92	0.00006	0.23	0.00006
1.12	0.000443	0.55	0.000443
0.25	0.00107	0.91	0.00107

Table 3. Material properties

Type	Compressive strength (MPa)	Yield strength (MPa)	Ultimate tensile strength (MPa)	Young's modulus (GPa)	Poisson's ratio
Concrete	25	-	-	20	0.2
Steel	-	400	600	200	0.3
CFRP	-	-	1721	130	0.3
Epoxy	-	-	6	3.1	-

Table 4. Numerical results.

Models	Ultimate load, P_y (kN)	Increase in load vs CSW (%)	Yield displacement, Δ_y (mm)	Ultimate displacement, Δ_u (mm)	Increase in displacement vs CSW (%)	Ductility, μ	Energy absorption (kN.mm)
CSW	101.8	0	7.09	18.4	0	2.59	1512
SSW-CF1-1L	121.8	19.5	6.99	19.8	7.6	2.83	2010
SSW-CF1-2L	127.3	25	7.06	18.4	0	2.6	1886
SSW-CF2-1L	122.5	20	8.5	21.5	16.8	2.51	2125
SSW-CF2-2L	101.9	0.1	7.77	18.4	0	2.36	1647
SSW-CF3-1L	127.7	25.4	7.23	19.8	7.6	2.73	2041
SSW-CF3-2L	137.2	34.7	9.83	23.1	25.5	2.34	2618
SSW-CF4-1L	101.8	0	6.94	18.4	0	2.63	1518
SSW-CF4-2L	117.5	15.4	7.6	18.4	0	2.42	1738
SSW-ST1	126.6	24.3	9.66	21.5	16.8	2.22	2110
SSW-ST2	173.2	70	6.87	21.5	16.8	3.12	3073
SSW-ST3	156.5	53.7	7.26	23.1	25.5	3.18	3031
SSW-ST4	119.8	17.6	7.5	21.5	16.8	2.86	2090